Journal of Thermal Science Vol.30, No.3 (2021) 807−816

https://doi.org/10.1007/s11630-020-1322-2 **Article ID: 1003-2169(2021)03-0807-10**

Thermal-Hydraulic Calculation and Analysis on Evaporator System of a 1000 MW Ultra-Supercritical Pulverized Combustion Boiler with Double Reheat

WAN Li, YANG Dong*, ZHOU Xihong, DONG Le, LI Juan

State Key Laboratory of Multiphase Flow in Power Engineering, Xi'an Jiaotong University, Xi'an 710049, China

Abstract: A double reheat ultra-supercritical boiler is an important development direction for high-parameter and large-capacity coal-fired power plants due to its high thermal efficiency and environmental value. China has developed a 1000 MW double reheat ultra-supercritical boiler with steam parameters of 35 MPa at 605°C/613°C/613°C. Reasonable water wall design is one of the keys to safe and reliable operation of the boiler. In order to examine the thermal-hydraulic characteristics of the double reheat ultra-supercritical boiler, the water wall system was equivalent to a flow network comprising series-parallel circuits, linking circuits and pressure nodes, and a calculation model was built on account of the conservation equations of energy, momentum and mass. Through the iterative solving of nonlinear equations, the prediction parameters of the water wall at boiler maximum continue rate (BMCR), 75% turbine heat-acceptance rate (THA) and 30% THA loads, including total pressure drops, flow distribution, outlet steam temperatures, fluid and metal temperatures were gotten. The results of calculation exhibit excellent thermal-hydraulic characteristics and substantiate the feasibility of the water wall design of the double reheat ultra-supercritical boiler.

Keywords: double reheat, ultra-supercritical boiler, water wall, flow network method, thermal-hydraulic characteristic

1. Introduction

A double reheat ultra-supercritical boiler, which is an important clean coal power generating technology, can considerably improve the boiler thermal efficiency, cut down fuel consumption, and decrease pollutants and waste streams [1–4]. Therefore, this development direction is important for the sustainable growth of China electricity industry [5, 6] and has been identified as the national key research and development program during the twelfth five-year plan period [7]. High-temperature water wall tube materials should be applied in the double reheat ultra-supercritical boiler due to complicated temperature regulation, low main steam flow, high fluid temperature of water wall, and metal temperature. The peak shaving mode is generally adopted by variable pressure. Thus, when the unit changes rapidly from low load to rated load, the operating pressure of the boiler changes in the range from subcritical to ultra-supercritical, and problems such as pulsation among tubes, hydrodynamic multi-values, and flow instability may occur. Therefore, thermal-hydraulic characteristics calculation of the double reheat ultra-supercritical boiler must be considered in the design and safe operation of the water wall.

Domestic and foreign scholars have carried out comprehensive and in-depth research on thermal-hydraulic calculation of pulverized combustion boilers by

Received: Jul 02, 2019 AE: LIU Zhijian Corresponding author: YANG Dong E-mail: dyang@mail.xjtu.edu.cn

Nomenclature

d_n	inner diameter/m	Re_b	Reynodes number while the qualitative temperature is bulk fluid temperature
d_w	outer diameter/m	Re_g	Reynodes number of the gas phase
f	friction coefficient	Re_w	Reynodes number while the qualitative temperature is inner tube wall temperature
G	mass flux/kg·m^{-2}·s^{-1}	s	tube pitch/m
h	enthalpy/J·kg^{-1}	T_f	fluid temperature/°C
h_f	enthalpy of bulk fluid/J·kg^{-1}	T_m	metal temperature in the middle of tube wall/°C
h_{in}	inlet enthalpy/J·kg^{-1}	T_n	metal temperature of inner tube wall/°C
h_{out}	outlet enthalpy/J·kg^{-1}	T_{qd}	metal temperature in the tip of fin/°C
h_w	enthalpy of fluid of tube wall surface fluid/J·kg^{-1}	T_{qg}	metal temperature in the root of fin/°C
J_n	non-uniformity coefficient of heat flux of inner wall	T_w	metal temperature of outer tube wall/°C
k	absolute roughness of the inner tube/m	x	steam quality of fluid/kg·kg^{-1}
l	tube length/m	**Greek symbols**	
$M(i)$	mass flow rate in circuit i/kg·s^{-1}	α	coefficient of heat transmission/ kW·m^{-2}·°C^{-1}
M_{tot}	total mass flow rate/kg·s^{-1}	δ	fin thickness/m
Nu	Nusselt number	η_{qd}	balance coefficient of heat flux in the tip of fin
$P(i)$	pressure in circuit i/MPa	η_{qg}	balance coefficient of heat flux in the root of fin
P_{cs}	outlet pressure in economizer/MPa	λ	thermal conductivity of tube/W·m^{-1}·K^{-1}
$\Delta P(i)$	pressure drop in circuit i/MPa	λ_{cr}	critical thermal conductivity /W·m^{-1}·K^{-1}
ΔP_f	frictional pressure drop/MPa	λ_g	thermal conductivity of the gas phase/ W·m^{-1}·K^{-1}
ΔP_g	gravitational pressure drop/MPa	μ_w	dynamic viscosity while the qualitative temperature is inner tube wall temperature/ N·s·m^{-2}
ΔP_l	local pressure drop/MPa	ξ	local resistance coefficient
Pr_b	Prandtl number of while the qualitative temperature is bulk fluid temperature	ρ	average density of fluid/kg·m^{-3}
Pr_{gw}	Prandtl number of the gas phase while the qualitative temperature is inner tube wall temperature	ρ_g	density of gas phase/kg·m^{-3}
Pr_w	Prandtl number while the qualitative temperature is inner tube wall temperature	ρ_l	density of liquid phase/kg·m^{-3}
$\overline{Pr_w}$	Average Prandtl number while the qualitative temperature is inner wall temperature	ρ_w	density while the qualitative temperature is inner tube wall temperature/kg·m^{-3}
q	heat flux/W·m^{-2}	ψ	correction coefficient
q_w	heat flux of outer wall/W·m^{-2}		

using different model buildings to examine the performance in the design of the boiler evaporator system. Thermal-hydraulic calculation model of boilers has developed from the complex graphical method with low precision to the simplified flow network method applied in computers. Tucakovic et al. [8] established a calculation method suitable for drum boilers and analyzed the water circulation safety of a rifled water wall at different loads. Adam and Marchetti [9], and Kim and Choi [10] proposed a calculation method based on homogeneous model for drum water level and mass distribution of a water circulation system of natural circulation boiler system. Dong et al. [11] presented a thermal-hydraulic circuit analysis method that can directly calculate hydraulic characteristics of each tube in each circuit of a natural circulation boiler. Zhao [12] put forward a universal hydrodynamic calculation model applicable to drum boilers. The above-mentioned references indicate that all these studies focus on mathematical models suitable for drum boilers. For research on the once-through boiler, Zhang et al. [13] analyzed hydrodynamic characteristics of vertical tubes

in supercritical pulverized coal boiler. According to the energy, mass and momentum conservations, Pan et al. [14] developed a flow network method suitable for supercritical once-through boilers. These works are all carried out on the pulverized coal boiler. Compared with single reheat pulverized coal boiler, the more reliable material applied in the evaporator system of the double reheat pulverized coal boiler is required. Thus, research on the thermal-hydraulic calculation of the double reheat boiler is important. A thermal-hydraulic calculation model of the ultra-supercritical boiler is developed in this study on account of three conservation laws, and validated empirical heat transfer correlations are embedded in the calculation model to present and analyze the prediction parameters of water wall.

2. Water Wall Structure and Circuit Division

The furnace of the 1000 MW double reheat ultra-supercritical boiler is approximately 20.76 m wide, 20.76 m deep, and 114 m high. There are two stages of the water wall system. The spiral smooth water wall is in the first stage and the vertical smooth water wall is in the second stage. The lower water wall with spiral tubes consists of 692 tubes of Φ 38 mm, whereas the upper water wall with vertical tubes comprises two parts. The upper water wall consists of 1384 tubes of Φ 38 mm at the lower part, and every two vertical tubes merge into one tube. Thus, at the upper part, the upper water wall consists of 692 tubes of Φ 44.5 mm. Table 1 summarizes the operating parameters of water wall.

Table 1 Operating parameters of water wall

Parameter	BMCR	75%THA	30%THA	Unit
Total mass flow rate	2608	1766	782	t/h
Inlet temperature	361	345	316	°C
Inlet pressure	37.12	24.98	10.96	MPa
Outlet temperature	482	449.2	386	°C
Outlet pressure	35.42	24.15	10.8	MPa

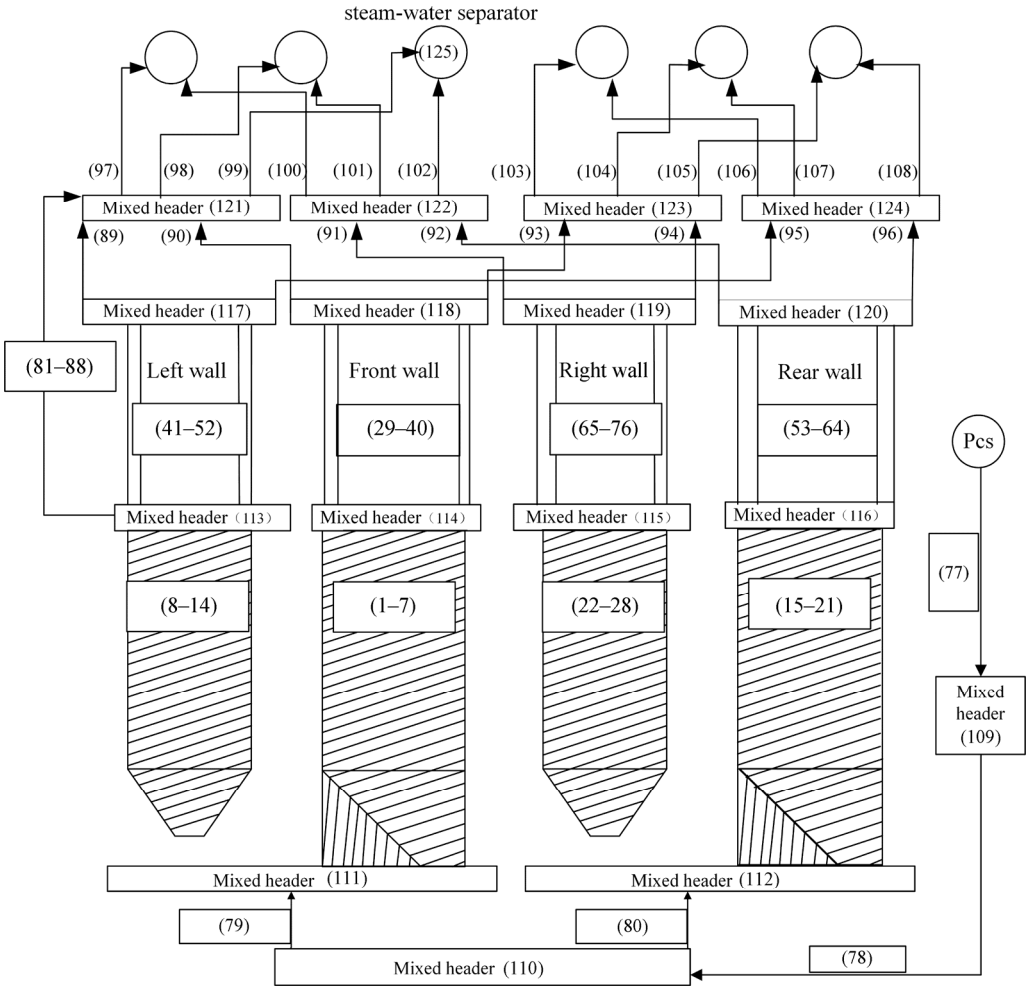

Fig. 1 Flow network system

Series-parallel circuits, linking circuits and pressure nodes are contained in the flow network system showed in Fig. 1, representing the vertical and spiral tubes, linking tubes, and headers of the ultra-supercritical boiler. As shown in Fig. 1, there are 76 heated circuits, 32 unheated linking circuits and 17 pressure nodes, and the sequence numbers 1–28 and 29–76 represent heated circuits in the lower and upper walls. The unheated linking tubes, various headers, and steam-water separator are represented by the sequence numbers 77–108, 109–124, and 125, respectively.

On the basis of furnace heat equilibrium [15], the heat flux distribution along the furnace height direction of the double reheat ultra-supercritical boiler is obtained, which is shown in Fig. 2. As shown in the figure, the heat flux along the furnace height increases with the increase of operating load, which is reasonable. For the purpose of analyzing the effect of the heat flux non-uniformity in horizontal direction on mass flow rate and metal temperatures, the heat flux deviation at level direction should be considered. According to characteristics of corner tangential combustion mode, combined with related research results of numerical simulation, the non-uniformity coefficient of heat flux along the width direction of the furnace is given in Fig. 3, which has been proved to be simulated well in actual furnace. Observed in Fig. 3, the heat flux deviation curve is analyzed counterclockwise (overlooking) along the furnace width of each wall.

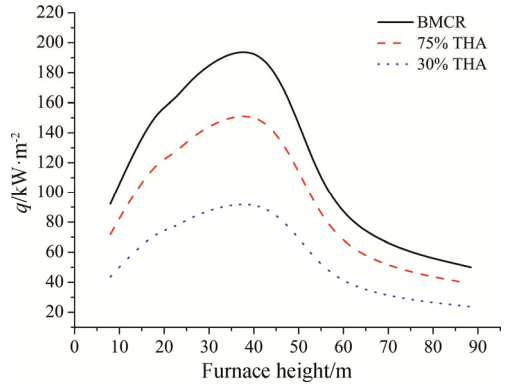

Fig. 2 Heat flux distribution along the furnace height direction

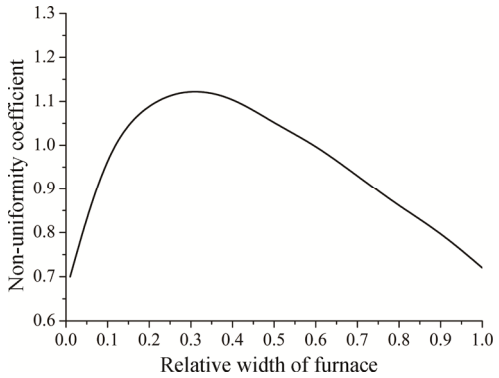

Fig. 3 Non-uniformity coefficient of heat flux along the width direction of the furnace

3. Mathematical Model

3.1 Analysis model of pressure drop and mass flow

For the purpose of predicting the pressure drop between nodes and the mass flux of circuits, a calculation model is established on account of mass and momentum conservations. This model consists of 125 equations, which can be simultaneously solved by iteration method [16].

For 76 heated circuits and 32 unheated linking circuits, the momentum conservation equations are presented as:

$$0 = P(\text{innode}) - P(\text{outnode}) - \Delta P(i) \quad (1 \le i \le 108) \quad (1)$$

where the in-node number and out-node number can be observed in Fig. 1. For example, the momentum conservation equations of circuits in lower front wall and linking circuit 77 are given as

$$0 = P(111) - P(114) - \Delta P(i) \quad (1 \le i \le 7) \quad (2)$$

$$0 = P_{cs} - P(109) - \Delta P(77) \quad (3)$$

The mass conservation equations of pressure nodes are presented as:

$$0 = \sum [M(i)_{in}] - \sum [M(i)_{out}] \quad (1 \le i \le 108) \quad (4)$$

For example, the mass conservation equations of pressure nodes 110, 112 and 115 are given respectively as

$$0 = \sum_{i=79}^{80} M(i) - M(78) \quad (5)$$

$$0 = \sum_{i=15}^{28} M(i) - M(80) \quad (6)$$

$$0 = \sum_{i=65}^{76} M(i) + \sum_{i=87}^{88} M(i) - \sum_{i=22}^{28} M(i) \quad (7)$$

The total pressure drops are affected by the vertical height difference between inlet and outlet position, the friction between fluid and inner tube wall, local resistance and accelerated pressure drop. Because the accelerated pressure drops account for a small proportion of total pressure drops and have little effect on calculation results, the total pressure drops in circuit i without the consideration of the accelerated pressure drops can be confirmed as:

$$\Delta P(i) = \Delta P_g(i) + \Delta P_f(i) + \Delta P_l(i) \quad (8)$$

The gravitational pressure drops are associated with the density of fluid and vertical height difference between inlet and outlet position, which are calculated as:

$$\Delta P_g = \rho g h \quad (9)$$

The frictional pressure drops of single-phase water in

smooth tubes are given as:

$$\Delta P_{\mathrm{f}} = f\frac{l}{d_{\mathrm{n}}}\frac{G^2}{2\rho} \tag{10}$$

The frictional pressure drops of two-phase steam-water in smooth tubes are given by [15]:

$$\Delta P_{\mathrm{f}} = \psi f\frac{l}{d_{\mathrm{n}}}\frac{G^2}{2\rho_{\mathrm{l}}}\left[1+x\left(\frac{\rho_{\mathrm{l}}}{\rho_{\mathrm{g}}}-1\right)\right] \tag{11}$$

where the correction coefficient ψ is calculated as:

$$\psi = 1,\quad G = 1000\ \mathrm{kg/(m^2\cdot s)}; \tag{12}$$

$$\psi = 1+\frac{x(1-x)\left(\dfrac{1000}{G}-1\right)\dfrac{\rho_{\mathrm{l}}}{\rho_{\mathrm{g}}}}{1+x\left(\dfrac{\rho_{\mathrm{l}}}{\rho_{\mathrm{g}}}-1\right)}, \tag{13}$$

$$G < 1000\ \mathrm{kg/(m^2\cdot s)};$$

$$\psi = 1+\frac{x(1-x)\left(\dfrac{1000}{G}-1\right)\dfrac{\rho_{\mathrm{l}}}{\rho_{\mathrm{g}}}}{1+(1-x)\left(\dfrac{\rho_{\mathrm{l}}}{\rho_{\mathrm{g}}}-1\right)}, \tag{14}$$

$$G > 1000\ \mathrm{kg/(m^2\cdot s)};$$

In the above equations, the friction coefficient f is given with the absolute roughness of the inner tube wall k and the value of k for carbon steel in this study is 6×10^{-5}, whose formula is given by:

$$f = \frac{1}{4\left[\lg\left(\dfrac{3.7d_{\mathrm{n}}}{k}\right)\right]^2} \tag{15}$$

The correlations of local pressure drops for single-phase water and two-phase steam-water in smooth tubes, which are estimated by elbows, inlet and outlet structure, are confirmed respectively by [15]:

$$\Delta P_{\mathrm{l}} = \xi\frac{G^2}{2\rho} \tag{16}$$

$$\Delta P_{\mathrm{l}} = \xi\frac{G^2}{2\rho_{\mathrm{l}}}\left[1+x\left(\frac{\rho_{\mathrm{l}}}{\rho_{\mathrm{g}}}-1\right)\right] \tag{17}$$

Energy conservation equation, whose thermodynamic parameters are related to the mass flow rate and the heat flux along height, can be presented as:

$$h_{\mathrm{out}} = h_{\mathrm{in}} + \frac{qsl}{M_{\mathrm{tot}}} \tag{18}$$

3.2 Analysis model of metal temperatures

For the calculation model of metal temperatures, the heat transfer coefficient is a key factor. Through experimental investigation on heat transfer characteristics of spiral and vertical smooth tubes, the validated correlations of heat transfer coefficient are obtained.

(1) Heat transfer coefficient of spiral smooth tubes

Under supercritical pressure, the validated average heat transfer coefficient of spiral smooth tubes is proposed [17].

$$Nu = 0.004\ 59Re_{\mathrm{w}}^{0.923}\overline{Pr}_{\mathrm{w}}^{0.613}\left(\frac{\rho_{\mathrm{w}}}{\rho}\right)^{0.231} \tag{19}$$

Under subcritical pressure, the heat transfer coefficient is proposed as [17]:

$$Nu = 0.021Re_{\mathrm{b}}^{0.8}Pr_{\mathrm{b}}^{0.43}\left(\frac{Pr_{\mathrm{b}}}{Pr_{\mathrm{w}}}\right)^{0.25} \tag{20}$$

(2) Heat transfer coefficient of vertical smooth tubes

Under supercritical pressure, the validated heat transfer coefficients of vertical smooth tubes in the low and high enthalpy are presented [18].

In the low-enthalpy region:

$$Nu = 35.21Re_{\mathrm{w}}^{0.654}\left(\frac{h_{\mathrm{w}}-h_{\mathrm{f}}}{T_{\mathrm{w}}-T_{\mathrm{f}}}\cdot\frac{\mu_{\mathrm{w}}}{\lambda}\right)^{0.841}\left(\frac{\rho_{\mathrm{w}}}{\rho}\right)^{0.281} \tag{21}$$

In the high-enthalpy region:

$$Nu = 246.6Re_{\mathrm{w}}^{0.351}\left(\frac{h_{\mathrm{w}}-h_{\mathrm{f}}}{T_{\mathrm{w}}-T_{\mathrm{f}}}\cdot\frac{\mu_{\mathrm{w}}}{\lambda}\right)^{0.453}\left(\frac{\rho_{\mathrm{w}}}{\rho}\right)^{0.361} \tag{22}$$

Under critical pressure, the heat transfer coefficient in normal region can be found in Ref. [15] and that in heat transfer deterioration region is proposed as [19]:

$$Nu = 0.000\ 149\left\{Re_{\mathrm{g}}\left[x+\frac{\rho_{\mathrm{g}}}{\rho_{\mathrm{l}}}(1-x)\right]\right\}^{0.459} \times Pr_{\mathrm{gw}}^{0.463}q^{1.531}\left(\frac{\lambda_{\mathrm{g}}}{\lambda_{\mathrm{cr}}}\right)^{0.803} \tag{23}$$

Under subcritical pressure, the heat transfer coefficient correlations of vertical smooth tubes are given by Ref. [15].

The temperatures of inner and outer tube wall are given by [15]

$$T_{\mathrm{n}} = T_{\mathrm{f}} + J_{\mathrm{n}}\frac{q_{\mathrm{w}}}{\alpha}\frac{d_{\mathrm{w}}}{d_{\mathrm{n}}} \tag{24}$$

$$T_{\mathrm{w}} = T_{\mathrm{f}} + J_{\mathrm{n}}\frac{q_{\mathrm{w}}}{\alpha}\frac{d_{\mathrm{w}}}{d_{\mathrm{n}}} + Jq_{\mathrm{w}}\frac{2d_{\mathrm{w}}\left(d_{\mathrm{w}}-d_{\mathrm{n}}\right)}{\lambda\left(d_{\mathrm{w}}+d_{\mathrm{n}}\right)} \tag{25}$$

The mid-wall temperatures are confirmed by

$$T_{\mathrm{m}} = \frac{T_{\mathrm{n}}+T_{\mathrm{w}}}{2} \tag{26}$$

The temperatures in the root of fin can be obtained on the basis of heat transfer principle [20]. The formula is presented by

$$T_{\mathrm{qg}} = T_{\mathrm{f}} + q_{\mathrm{w}}\eta_{\mathrm{qg}}\frac{d_{\mathrm{w}}}{d_{\mathrm{n}}}\left[\ln\left(\frac{d_{\mathrm{w}}}{d_{\mathrm{n}}}\right)\frac{d_{\mathrm{n}}}{2\lambda}+\frac{1}{\alpha}\right] \tag{27}$$

The temperatures in the tip of fin are calculated by [14]

$$T_{\mathrm{qd}} = T_{\mathrm{qd}} + \frac{q\eta_{\mathrm{qd}}}{2\lambda\delta}\left(\frac{s-d_{\mathrm{w}}}{2}\right)^2 \tag{28}$$

3.3 Model validation

A mathematical model for analyzing the thermal-hydraulic performance of a same type supercritical once-through boiler put into operation is proposed in Ref. [21], which is similar with the model in this study. In order to verify the correctness and reliability of the model, comparison between calculated value and furnace data of the boiler in Ref. [21] is given, and comparison of the temperature profiles of outlet steam in the lower furnace at BMCR load and that in the upper furnace at 75% BMCR load are shown in Fig. 4 and Fig. 5, respectively [21]. Observed in the figures, the calculated values of the outlet steam temperature in the lower and upper furnaces are consistent with the distribution trends of the furnace data. Since the heat flux distribution during actual operation are affected by the coal type, the operation mode and the slagging situation, there is a difference between the curve of actual furnace and calculation, and the difference between the actual furnace geometry and the calculation structure, all of which can cause deviation of calculated value and furnace data. Moreover, the difference between calculated value and furnace data is no more than 2%, indicating that the thermal-hydraulic mathematical model is correct and reliable.

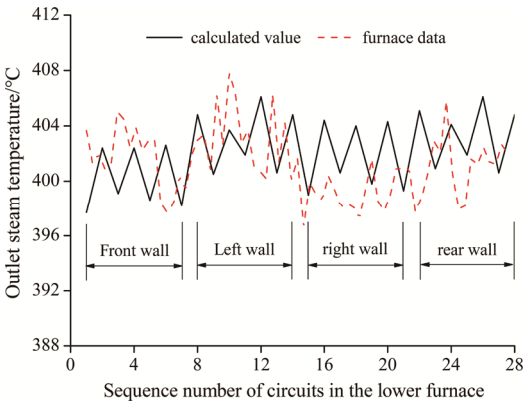

Fig. 4 Comparison of temperature profiles of outlet steam in the lower furnace

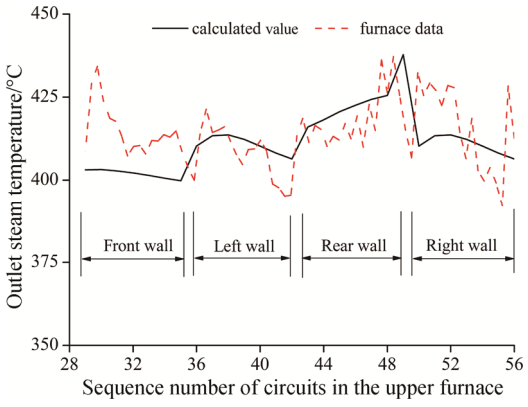

Fig. 5 Comparison of temperature profiles of outlet steam in the upper furnace

4. Prediction Results and Discussion

4.1 Total pressure drops

At different operating loads, the total pressure drops (from inlet header to steam separator) of the ultra-supercritical boiler are summarized in Table 2. As shown in the Table, the total pressure drops decrease with the decrease of operating load.

Table 2 Total pressure drops in water wall

Load	Total pressure drop/MPa
BMCR	2.307
75%THA	1.472
30%THA	0.77

4.2 Flow distribution

Figure 6 exhibits the flow distribution of lower spiral water wall. The circuits are evenly heated because of coming around the furnace with uniform high and low heat fluxes, and the different tube lengths in the water wall have an effect on the flow distribution. Given that the lengths of tubes in circuits 4, 5, 11, 12, 18, 19, 25 and 26 that pass around the burner area are longer than those of the tubes in other circuits, the mass fluxes in these circuits are smaller. For BMCR rate, the mass flux in circuit 22 of 2425 kg/(m^2·s) is the largest, whereas the mass flux in loop 19 of 2090.1 kg/(m^2·s) is the smallest. As a result, the maximum mass flux difference is 13.8%. For 75% THA rate, the maximum and minimum flows appear in circuits 2 and 19, respectively. The mass flux range is 1386 to 1661.9 kg/(m^2·s), and the maximum mass flux difference is 16.6%. For 30% THA rate, the maximum and minimum flows appear in circuits 1 and 19, respectively. The mass flux range is 592.6 to 751.7 kg/(m^2·s), and the maximum mass flux deviation is 21.2%.

Figure 7 exhibits the flow distribution of upper vertical water wall. The horizontal heat flux deviation is the main factor causing flow differences in circuits of each wall along the width direction of the furnace. Moreover, the mass flux of the circuit with high heat absorption is small, that is, the mass flux has a negative response to the heat flux. This condition means that the frictional pressure drop becomes the main flow resistance in upper vertical water wall and the disturbance increases with the increasing of heat flux, which augment frictional resistance. The mass fluxes in the front and left walls are similar to those in the back and right walls, respectively. As observed in Fig. 7, it indicates that the mass flux difference is relatively small in the upper furnace and flow differences increase with the increase of load. For BMCR rate, the mass flux in circuit 66 of 1283.4 kg/(m^2·s) is the largest, whereas the mass flux in circuit

61 of 1229.1 kg/(m^2·s) is the smallest. Thus, the maximum mass flux deviation is 4.2%. At 75% THA load, the maximum and minimum mass fluxes appear in circuits 66 and 49, respectively. The maximum mass flux deviation under this load is 4.8%. For 30% THA load, the maximum and minimum fluxes appear in circuits 30 and 49, respectively. The maximum mass flux deviation under this load is 5.7%.

4.3 Outlet steam temperature

The temperature profile of outlet steam in the lower furnace is shown in Fig. 8. In the lower furnace, negative response characteristics between mass flow and outlet steam temperature are observed (Fig. 8). In particular, a circuit with high outlet steam temperature draws less mass flux. For instance, as the results of BMCR rate, the outlet steam temperature in circuit 19 with the smallest mass flux is the highest at 451.7°C and that in circuit 22 with the largest mass flux is the lowest at 439.9°C. It indicates that the outlet steam temperature decreases with the decrease of the load. For 75% THA rate, the maximum and minimum outlet steam temperatures are respectively 412.7°C and 394.9°C. For 30% THA rate, the maximum and minimum outlet steam temperatures are respectively 335.4°C and 317.9°C. In general, the outlet steam temperature deviation of spiral wall tubes in the lower furnace is small. The reason is that the circuits of spiral tubes pass around the regions with large and small heat absorption deviations at the same time. Moreover, the heat absorption of each circuit is relatively close, which is a major advantage of spiral tubes.

The temperature profile of outlet steam in the upper furnace is shown in Fig. 9. For upper water wall, the temperature deviation of outlet steam is larger than that of lower water wall due to different heat absorption deviations of each circuit of vertical tubes. The vertical tubes that are heated strongly absorb a large amount of heat, and this condition increases the fluid temperature. The maximum and minimum outlet steam temperatures appear on the left and front walls, respectively. At BMCR load, the maximum temperature deviation of outlet steam is 35.3°C. As the results of this load, the outlet steam temperature is the highest at 510.8°C but within the allowable temperature of boiler operation. At 75% THA

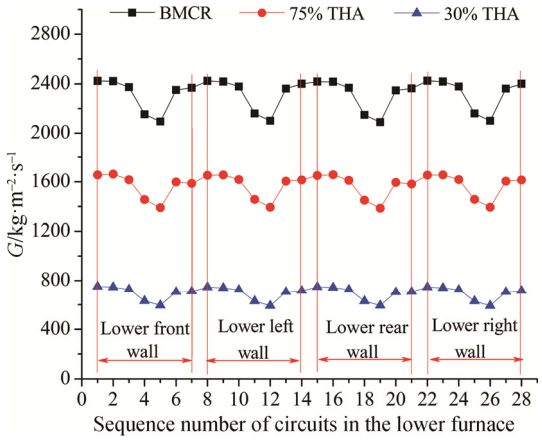

Fig. 6 Flow distribution of lower spiral water wall

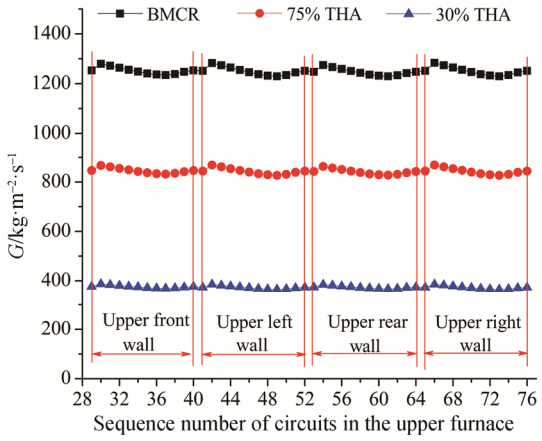

Fig. 7 Flow distribution of upper vertical water wall

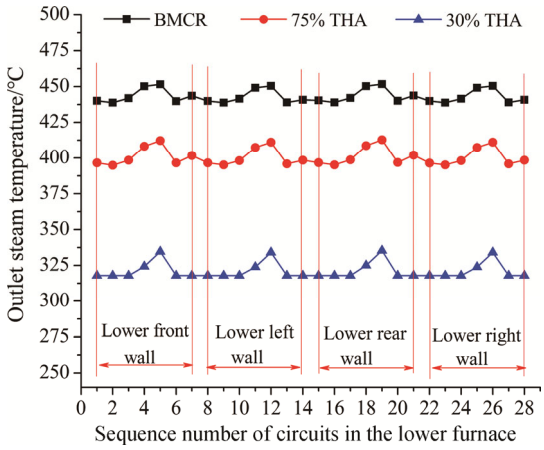

Fig. 8 Temperature profiles of outlet steam in the lower furnace

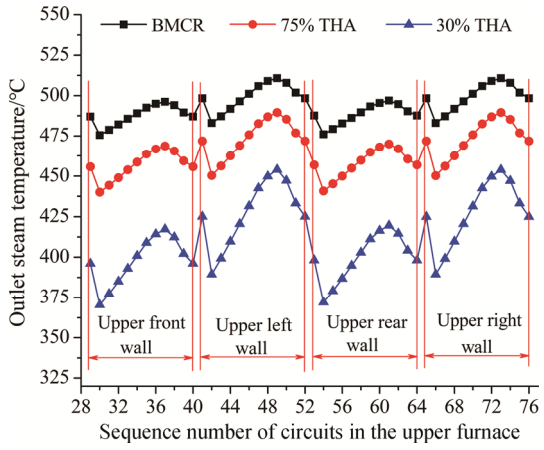

Fig. 9 Temperature profiles of outlet steam in the upper furnace

load, the maximum and minimum outlet steam temperatures are 489.6°C and 440°C, respectively. The temperature difference under this load is 49.6°C. The maximum and minimum outlet steam temperatures under 30% THA load are respectively 454°C and 370.3°C, so the maximum temperature deviation is 83.7°C. The influence of heat fluxes on outlet steam temperature can be significantly improved by the low mass flow. Thus, the temperature deviation of outlet steam with low mass flux under 30% THA load is the largest, but it meets safety requirements.

4.4 Fluid and metal temperatures

For BMCR rate, the temperature profiles of fluid and metal in the most dangerous circuits 5, 37, and 49 are exhibited in Figs. 10 to 12. Since the flow is in single-phase region, the fluid temperature rises with heat absorption. As observed in the longest circuit 5 of lower water wall, the metal temperatures increase as fluid temperature rises. Moreover, the maximum outer wall temperature reaches to 537.5°C at about 47 m of height. Due to high heat flux, the fluid and metal temperatures of upper water wall rise rapidly. Then, as the heat flux along height decreases, the metal temperatures decrease. The maximum outer wall and mid-wall temperatures are 546.7°C and 529°C, respectively, in circuit 49 in the upper wall. In addition, because some tube sections of spiral water wall are unheated tubes come around burner region, the metal temperature and fluid temperature becomes the same at some height in the lower furnace.

For 75% THA rate, the temperature profiles of fluid and metal in circuits 5, 37, and 49 are exhibited in Figs. 13–15. As shown in the figures, the metal temperature distribution is similar at BMCR and 75% THA loads. Since the flow is in large specific capacity region, the physical parameters vary sharply with the change in temperature. The temperature deviation between fluid and wall becomes larger when metal temperature is higher than the virtual critical temperature. As shown in Fig. 13, the metal temperatures of lower water wall increase as fluid temperature rises. Furthermore, the maximum outer wall temperature reaches to 478.9°C at 57 m of height. The maximum outer wall and mid-wall temperatures are 513.7°C and 503.5°C, respectively, in circuit 49 in the upper furnace.

For 30% THA rate, the temperature profiles of fluid and metal in circuits 5, 37, and 49 are exhibited in Figs. 16 to 18. Below 23.6 m, the fluid temperature increases monotonically in circuit 5 with furnace height rising in the lower water wall. When the furnace height reaches 23.6 m, the fluid temperature keeps constant because the flow enters the two-phase region. At the same time, the fluid coefficient of heat transmission increases evidently, causing the metal temperatures to decrease. At 31 m of height, the outer wall temperature of 435.9°C is the highest because of the maximum heat flux and dry-out occurs. At higher height of lower water wall, the metal temperatures along height decrease because the heat flux decreases. At 60 m of height, the fluid moves away from the two-phase region. Therefore, the temperatures of fluid and metal increase again with height rising. As observed in Figs. 17 and 18, it indicates that the temperatures of fluid and metal of upper water wall increase along height. The maximum outer wall and mid-wall temperatures are 463.9°C and 461.1°C, respectively, in circuit 49.

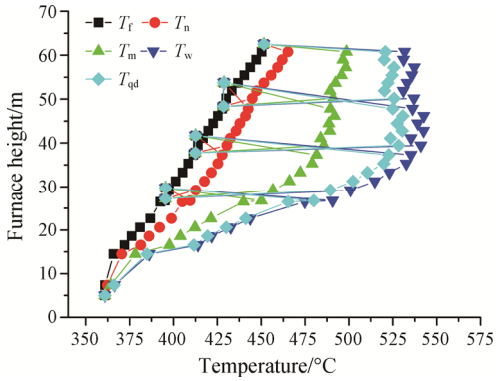

Fig. 10 Temperature profiles of fluid and metal in circuit 5 at BMCR load

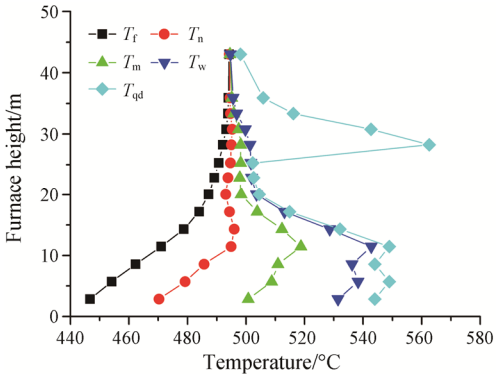

Fig. 11 Temperature profiles of fluid and metal in circuit 37 at BMCR load

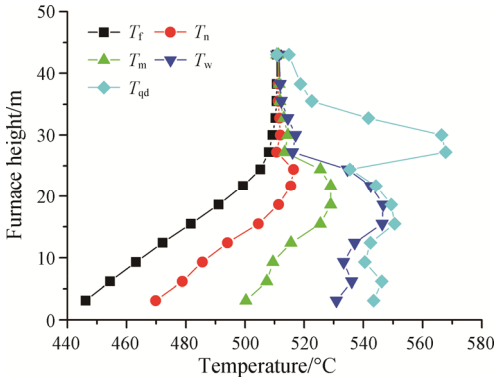

Fig. 12 Temperature profiles of fluid and metal in circuit 49 at BMCR load

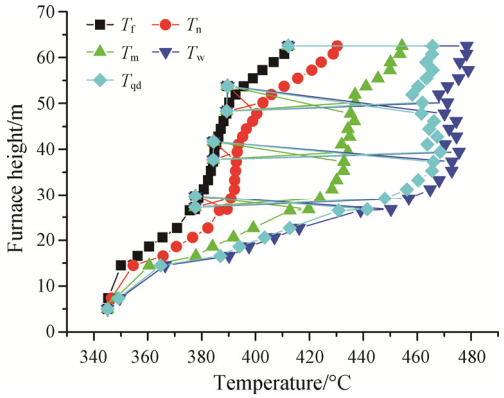

Fig. 13 Temperatures profiles of fluid and metal in circuit 5 at 75% THA load

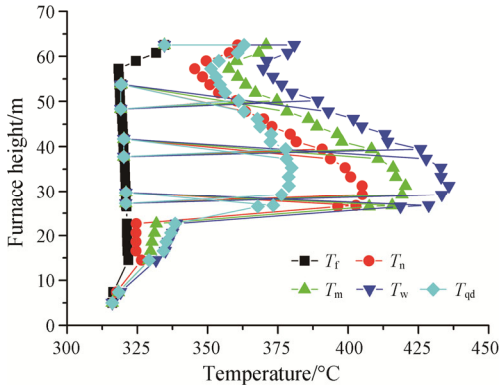

Fig. 16 Temperature profiles of fluid and metal in circuit 5 at 30% THA load

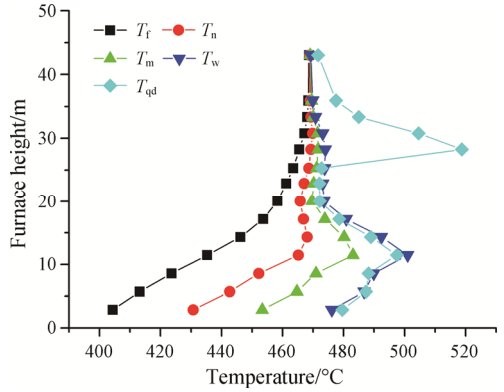

Fig. 14 Temperature profiles of fluid and metal in circuit 37 at 75% THA load

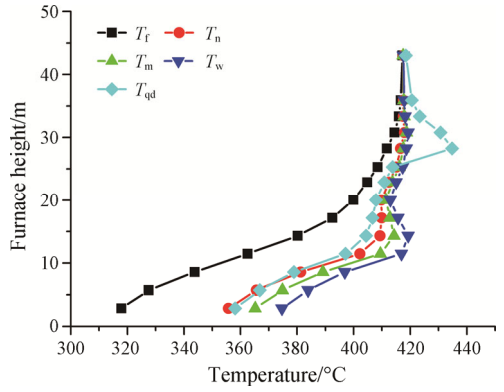

Fig. 17 Temperature profiles of fluid and metal in circuit 37 at 30% THA load

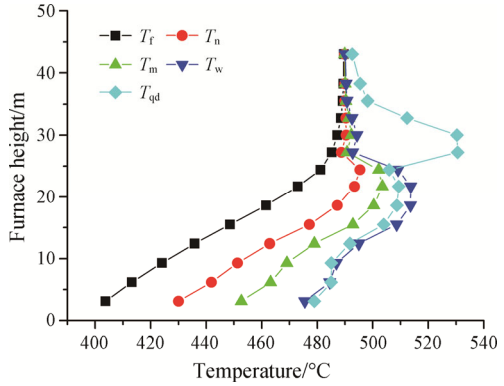

Fig. 15 Temperature profiles of fluid and metal in circuit 49 at 75% THA load

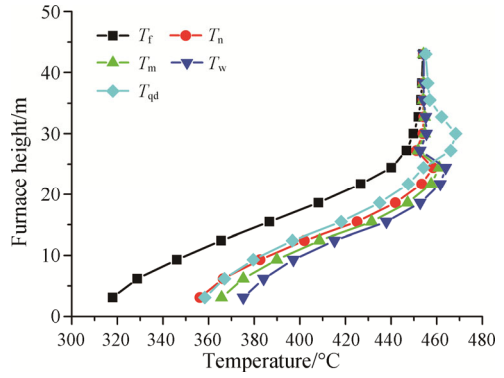

Fig. 18 Temperature profiles of fluid and metal in circuit 49 at 30% THA load

5. Conclusions

A thermal-hydraulic calculation model of the water wall system of a 1000 MW ultra-supercritical pulverized combustion boiler with double reheat was described in this study, and the total pressure drops, flow distribution, outlet steam temperatures, and temperatures of fluid and metal at different loads were calculated.

The results prove that the pressure drop and flow distribution characteristics are reasonable. The deviations of mass flux and outlet steam temperatures are both allowable. Meanwhile, the maximum temperatures of metal tube wall meet the operation requirements. The above-mentioned results exhibit excellent thermal-hydraulic characteristics, implying that the water wall design is feasible and reasonable.

Acknowledgement

This work is financially supported by the National Key Research & Development Program of China (2018YFB0604400).

References

[1] Xu G., Zhou L., Zhao S., et al., Optimum superheat utilization of extraction steam in double reheat ultra-supercritical power plants. Applied Energy, 2015, 160: 863–872.

[2] Xu G., Xu C., Yang Y., et al., Thermodynamic and economic analysis of a partially-underground tower-type boiler design for advanced double reheat power plants. Applied Thermal Engineering, 2015, 78(5): 565–575.

[3] Wang C., Qiao Y., Liu M., et al., Enhancing peak shaving capability by optimizing reheat-steam temperature control of a double-reheat boiler. Applied Energy, 2020, 260: 1–17.

[4] Si N., Zhao Z., Su S., et al., Exergy analysis of a 1000 MW double reheat ultra-supercritical power plant. Energy Conversion and Management. 2017, 147(3): 155–165.

[5] Li Y., Zhou L., Xu G., et al., Thermodynamic analysis and optimization of a double reheat system in an ultra-supercritical power plant. Energy, 2014, 74: 202–214.

[6] Yang D., Wang L., Bi Y., et al., Thermal-hydraulic analysis and metal temperature computation for the water wall of a 1000 MW ultra supercritical tower boiler with double reheat. Proceedings of the International Conference on Power Engineering: ICOPE, 2015. DOI: 10.1299/jsmeicope.2015.12._ICOPE-15-_121.

[7] Zhou L., Xu G., Zhao S., et al., Parametric analysis and process optimization of steam cycle in double reheat ultra supercritical power plants. Applied Thermal Engineering, 2016, 99: 652–660.

[8] Tucakovic D.R., Stevanovic V.D., Zivanovic T., et al., Thermal-hydraulic analysis of a steam boiler with rifled evaporating tubes. Applied Thermal Engineering, 2007, 27(2): 509–519.

[9] Adam E.J., Marchetti J.L., Dynamic simulation of large boilers with natural recirculation. Computers & Chemical Engineering, 1999, 23(8): 1031–1040.

[10] Kim H., Choi S., A model on water level dynamics in natural circulation drum-type boilers. International Communications in Heat and Mass Transfer, 2005, 32(6): 786–796.

[11] Dong P., Xu Y., Lan R., Loop analysis method for the numerical calculation of hydrodynamic characteristic of boiler with natural circulation. Journal of Harbin Institute of Technology, 2007, 39(3): 462–466. (in Chinese)

[12] Zhao Z., Universal model for hydrodynamic calculation. North China Electric Power, 2004, 12: 1–4. (in Chinese)

[13] Zhang D., Wu Y., Zhang H., et al., Hydrodynamic characteristics of vertical tubes with low mass flux in supercritical pulverized coal boiler. Proceedings of the CSEE, 2014, 34(32): 5693–5700. (in Chinese)

[14] Pan J., Yang D., Yu H., et al., Mathematical modeling and thermal-hydraulic analysis of vertical water wall in an ultra supercritical boiler. Applied Thermal Engineering, 2009, 29: 2500–2507.

[15] Wang M., Li Z., Dong Z., The national standard of the boiler hydrodynamics calculation (JB/Z201-83). Shanghai Power Equipment Packaged Design Research Institute, Shanghai, 1983. (in Chinese)

[16] David K., Ward C., Numerical analysis: mathematics of scientific computing. Brooks Publishing Company, CA, 2003.

[17] Wang S., Yang D., Zhao Y., et al., Heat transfer characteristics of spiral water wall tubes in a 1000 MW ultra-supercritical boiler with wide operating mode. Applied Thermal Engineering, 2018, 130: 501–514.

[18] Wang W., Liang Z., Wan L., et al., Experimental investigation on heat transfer characteristics of smooth water wall tube of an ultra-supercritical CFB boiler. Proceedings of the ASME 2018 International Mechanical Engineering Congress and Exposition: IMECE, 2018. Paper No: IMECE2018-86137, V08AT10A054.

[19] Wang W., Qu M., Zhao Y., et al., Experimental investigation on critical heat flux of smooth water wall tube with low mass flux at near-critical pressures. Proceedings of the CSEE, 2018, 38(10): 3015–3021. (in Chinese)

[20] Kakas S., Yener Y., Heat conduction. Second ed. Hemisphere Publishing Corporation, Washington, USA, 1986.

[21] Lu H., Yang D., Zhou X., et al., Calculation of pressure drop and outlet steam temperature of water wall pipes for supercritical once-through boiler. Journal of Xi'an Jiaotong University, 2011, 45(1): 38–42. (in Chinese)